CRYSTAL GROWTH & DESIGN

Article

Cite This: Cryst. Growth Des. XXXX, XXX, XXX−XXX

pubs.acs.org/crystal

Case Study of the Correlation between Metallogelation Ability and Crystal Packing

Hamid Reza Khavasi* and Maryam Esmaeili

Department of Inorganic Chemistry and Catalysis, Shahid Beheshti University, General Campus, Evin, Tehran 1983963113, Iran

Supporting Information

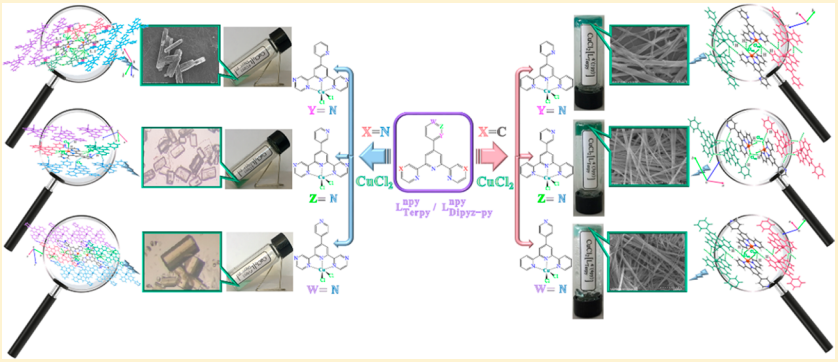

ABSTRACT: In the present paper, in order to find the correlation between the molecular structure and the intermolecular interaction patterns in the crystalline state and the corresponding gelating or nongelating behavior, two structurally related sets of copper complexes, including ($CuCl_2[L^{2py}_{Terpy}]$), **1**, ($CuCl_2[L^{3py}_{Terpy}]$), **2**, and ($CuCl_2[L^{4py}_{Terpy}]$), **3**, (where L^{npy}_{Terpy} is 4′-(*n*-pyridyl)-2,2′,6′,2″-terpyridine) as the first set and ($CuCl_2[L^{2py}_{dipyz\text{-}py}]$), **4**, ($CuCl_2[L^{3py}_{dipyz\text{-}py}]$), **5**, and ($CuCl_2[L^{4py}_{dipyz\text{-}py}]$), **6**, (where $L^{npy}_{dipyz\text{-}py}$ is 4-(*n*-pyridyl)-2,6-dipyrazin-2-yl-pyridine) as the second one, have been synthesized, and their crystal packing as well as gelating properties have been investigated. Results show that although these two sets are structurally similar the first set forms a metastable hydrogel, while the second one is unable to form a gel. To investigate the reasons, we employed Hirshfeld surface analysis and examined the differences in their packing arrangements, which suggest hydrogen bonding arranged into the three-dimensional network is a preferred mode of packing for the crystalline solid but is unfavorable for gel formation.

INTRODUCTION

Toward the rational design of low molecular weight gelators (LMWG) with new functional properties, noncovalent interactions such as hydrogen bonding, π-involved stacking, hydrophobic and hydrophilic effects, and charge transfer interactions have been utilized prevalently.[1−12] As plenty of gelators have been discovered serendipitously, persistent efforts have been made toward the rational design of new gelators.[13] LMWGs are the building blocks of supramolecular gels.[14] To rationally design of new molecules, it is essential to be informed of several molecular aspects such as the presence of different functional groups that can form linear chains through intermolecular interactions, which make compounds good candidates as building blocks for supramolecular gelation.[15−18] Lack of insight into the precise relationship between the structure of the assembly motif and the noncovalent interaction that construe the self-assembly process means the control of this aggregation phenomena is still a challenging goal.[14,15] Terpyridine derivatives have been shown to exhibit a significant ability to self-assemble into highly entangled fibrillar networks that prevent the flow of the bulk solvent and are able to immobilize and encapsulate solvent molecules,[19−27] thus leading to the gel-type macroscopic behavior. One of the approaches to finding the effective factors in the formation of fibers in the gel states is to select structures with similar variations and then investigate the behavior of their gelating ability with their single-crystal structure.[7,28,29] Different previous reports have shown that terpyridine-based complexes have a remarkable potential in the formation of gels; however, some of them do not have the potential of gel formation at all. The attributes of the ultimate gel will be controlled by the properties of the fibers that lead to the network also how the fibers cross-link or entangle and how the fibers are distributed in space. Correlation between the gel properties and network types is not reasonably well understood for very diverse gelating systems. To the best of our knowledge, reports on such linking between gel properties and network types are rare. In this regard, hydrogen-bonding supramolecular assembly in gelators are also reported.[30−32] Herein we used pyridine derivatives for such studies. All the terpyridine analogues reported herein are good gelators, whereas the corresponding dipyrazine-pyridine counterparts appear to have no gelation ability. To find the correlation between the gelation ability and the crystal structure, two series of copper complexes including

Received: January 24, 2019
Revised: June 9, 2019
Published: June 17, 2019

DOI: 10.1021/acs.cgd.9b00117
Cryst. Growth Des. XXXX, XXX, XXX−XXX

($CuCl_2[L^{2py}_{Terpy}]$), **1**, ($CuCl_2[L^{3py}_{Terpy}]$), **2**, and ($CuCl_2[L^{4py}_{Terpy}]$), **3**, (where L^{npy}_{Terpy} is 4′-(*n*-pyridyl)-2,2′,6′,2″-terpyridine) as the first series and ($CuCl_2[L^{2py}_{dipyz\text{-}py}]$), **4**, ($CuCl_2[L^{3py}_{dipyz\text{-}py}]$), **5**, and ($CuCl_2[L^{4py}_{dipyz\text{-}py}]$), **6**, (where $L^{npy}_{dipyz\text{-}py}$ is 4-(n-pyridyl)-2,6-dipyrazin-2-yl-pyridine) as the second series have been synthesized, Scheme 1. An attempt has been made for structure property correlations based on the single-crystal structures of the gelator molecules **1**−**3**, and the nongelators **4**−**6**. The crystal structures of **1**, **2**, **4**, and **5** intensity data were collected by single-crystal X-ray diffraction, Figure 1, in which we grew the single crystal from gelating solvents, and crystal structures of **3** (Refcode: OGOSOT)[33] and **6** (Refcode: EPELIW)[34] have been available and determined from the Cambridge Structural Database.[35] The aim of this work was to find the method that could help us correlate the intermolecular interaction patterns in the crystalline state and the gelling or nongelling behavior. We expected that this approach could explain the basic prerequisite for a terpyridine-based complex to be a good gelator.

Scheme 1. Molecular Structures of Synthesized Complexes

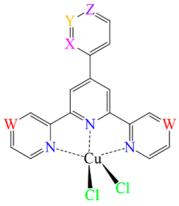

	Formula	W	X	Y	Z	Crystal	Gel
1	$CuCl_2[L^{2py}_{Terpy}]$	C	N	C	C	✓	✓
2	$CuCl_2[L^{3py}_{Terpy}]$	C	C	N	C	✓	✓
3	$CuCl_2[L^{4py}_{Terpy}]$	C	C	C	N	✓	✓
4	$CuCl_2[L^{2py}_{Dipyz\text{-}py}]$	N	N	C	C	✓	×
5	$CuCl_2[L^{3py}_{Dipyz\text{-}py}]$	N	C	N	C	✓	×
6	$CuCl_2[L^{4py}_{Dipyz\text{-}py}]$	N	C	C	N	✓	×

RESULTS AND DISCUSSION

The ligands were synthesized according to a literature method[36] by mixing of 2-acetylpyridine or 2-acetylpyridine and different pyridinaldehyde in ethanol at 2:1 molar ratio in the presence of KOH pellets and NH_3 solution. The reaction was completed by stirring the mixture at room temperature for 4 h. The corresponding complex was prepared by mixing of the same equivalents of these ligands and $CuCl_2{\cdot}2H_2O$ in methanol. For experimental details, see Supporting Information. The gelation ability of these compounds was examined in water by adopting the "stable to inversion of a test tube" method. The clear solution was achieved by dissolving a specific amount of complex in 1 mL of water under heating. The stable metallogel was formed by cooling of this solution down to room temperature. The water gelation behavior of all of these complexes was checked, and results showed that only complexes of the first series including ($CuCl_2[L^{2py}_{Terpy}]$), **1**, ($CuCl_2[L^{3py}_{Terpy}]$), **2**, and ($CuCl_2[L^{4py}_{Terpy}]$), **3**, (where L^{npy}_{Terpy} is 4′-(*n*-pyridyl)-2,2′,6′,2″-terpyridine) can be used as a gelator. Using water as a solvent, no gelating behavior for complexes of the second series including ($CuCl_2[L^{2py}_{dipyz\text{-}py}]$), **4**, ($CuCl_2[L^{3py}_{dipyz\text{-}py}]$), **5**, and ($CuCl_2[L^{4py}_{dipyz\text{-}py}]$), **6**, is observed. The T_{gel} values for these gels were measured by differential

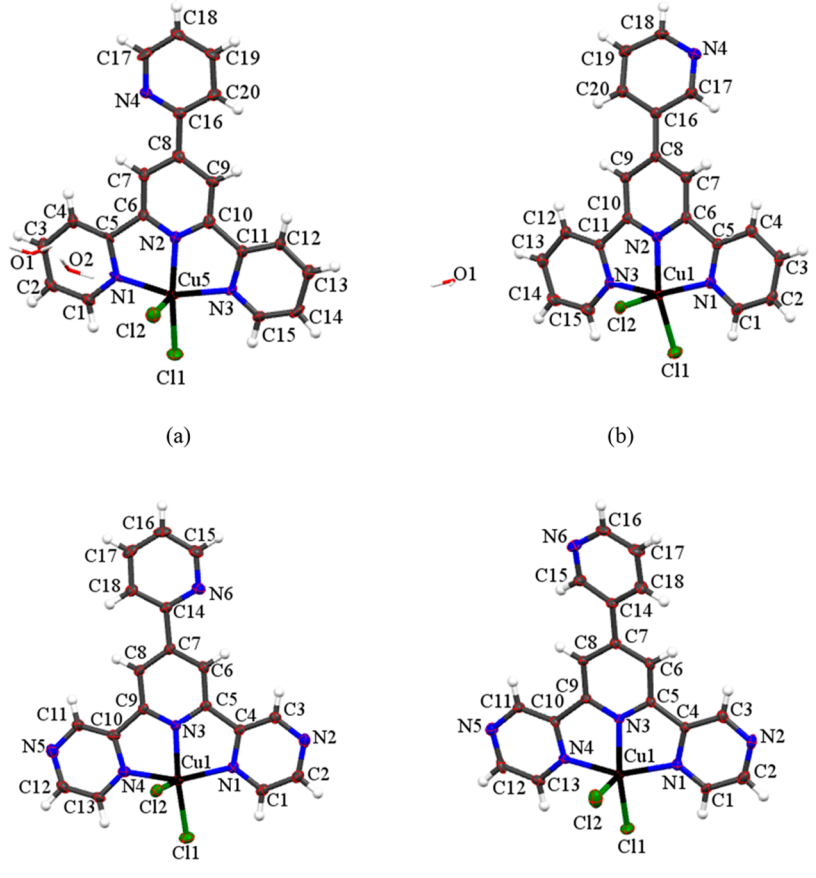

Figure 1. ORTEP diagrams of ($CuCl_2[L^{2py}_{Terpy}]$), **1** (a), ($CuCl_2[L^{3py}_{Terpy}]$), **2** (b), ($CuCl_2[L^{2py}_{dipyz\text{-}py}]$), **4** (c), and ($CuCl_2[L^{3py}_{dipyz\text{-}py}]$), **5** (d) at 30% ellipsoid probability that showing coordination geometry around the Cu(II) center. Solvent molecules are shown in stick form for better clarity.

DOI: 10.1021/acs.cgd.9b00117
Cryst. Growth Des. XXXX, XXX, XXX−XXX

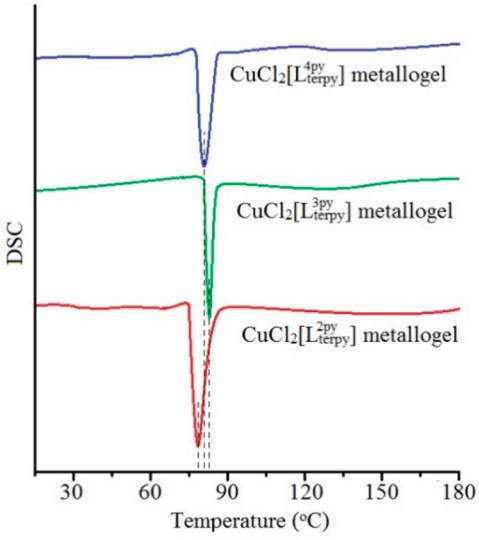

Figure 2. DSC data of the metallogels $CuCl_2[L^{2py}_{terpy}]$, $CuCl_2[L^{3py}_{terpy}]$, and $CuCl_2[L^{4py}_{terpy}]$ with a heating rate of 10 °C/min.

Compound	SEM image	Gel image	T_{gel}	MGC
$CuCl_2[L^{2py}_{terpy}]$	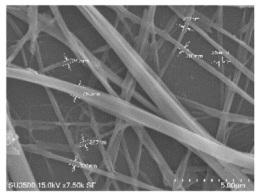		79	1.32
$CuCl_2[L^{3py}_{terpy}]$	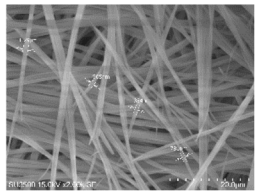		83	0.93
$CuCl_2[L^{4py}_{terpy}]$	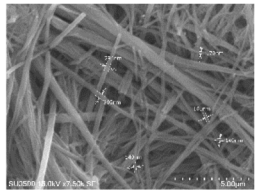		81	0.96

Figure 3. MGC, T_{gel}, gel images, and SEMs of xerogels from $CuCl_2[L^{2py}_{Terpy}]$, $CuCl_2[L^{3py}_{Terpy}]$, and $CuCl_2[L^{4py}_{Terpy}]$.

scanning calorimetry (DSC), Figure 2. For all gelators examined, an orderly rise in the sol−gel phase transition temperature T_{gel} was observed as the concentration of gelator molecules increased, which indicates the supramolecular nature of the gel forming network. $CuCl_2[L^{2py}_{Terpy}]$ had the lowest and $CuCl_2[L^{3py}_{Terpy}]$ the highest T_{gel} value at the same concentration in water, Figure 3. In general, the T_{gel} values of these compound increase in the order of $CuCl_2[L^{2py}_{Terpy}]$ < $CuCl_2[L^{4py}_{Terpy}]$ < $CuCl_2[L^{3py}_{Terpy}]$. SEM studies on the xerogel (vacuum-dried gel in 10^{-2} mbar at 5 min) of all the gelators show an entangled network of fine fibers. The position of nitrogen atom on the fourth ring of the ligand does not have a great effect on the microscopic structure of the gels. All the gels show numerous networks of fibrillar assemblies, and diameters of the tiniest detectable fibrils for each gel sample are 247, 50,

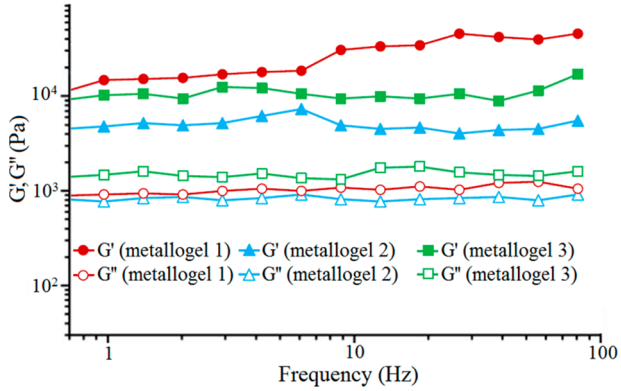

Figure 4. Elastic (storage) modulus, G', and loss modulus, G'', of the metallogels $CuCl_2[L^{2py}_{Terpy}]$ (**1**), $CuCl_2[L^{3py}_{Terpy}]$ (**2**), and $CuCl_2[L^{4py}_{Terpy}]$ (**3**) at different frequencies.

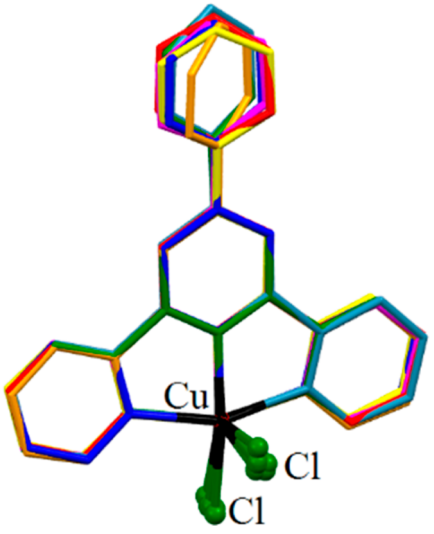

Figure 5. Overlay of the X-ray crystal structures of asymmetric units of complexes illustrates the conformational similarity.

and 161 nm for $CuCl_2[L^{2py}_{Terpy}]$, $CuCl_2[L^{3py}_{Terpy}]$, and $CuCl_2[L^{4py}_{Terpy}]$, respectively. The different gelation behaviors of gelators are reviewed in Figure 3. Overall, the more densely entangled fibrous gel network structure of these dried samples is in agreement with their higher thermal stability and intermolecular coherence, as represented by the T_{gel} values. Evaluation of viscoelastic properties of prepared metallogels is studied by rheology. The elastic (storage) modulus, G', and loss modulus, G'', rheological parameters at different frequencies are shown in Figure 4. As it is clear from this figure, typical gel-like rheological responses are displayed for all the cases. Note that the storage modulus G' is nearly independent of frequency and considerably higher than the loss modulus G'' showing the viscoelastic nature of the metallogels studied here.

To obtain a deeper understanding of the relevance between the molecular packing of the bulk crystalline state of a molecule and its gelation behavior, and for recognizing how the molecules pack in the fibers network in the gel state, single crystals of these complexes were determined by X-ray crystallography analysis. The crystal structures of **1**, **2**, **4**, and **5**, Figure 1, in which we grew the single crystal from gelating solvents have been refined, Table S1. Crystal structures of **3**

DOI: 10.1021/acs.cgd.9b00117
Cryst. Growth Des. XXXX, XXX, XXX−XXX

Table 1. Pairwise Structure Comparison of Geometrical Parameters of $CuCl_2[L^{npy}_{terpy}]$ and $CuCl_2[L^{npy}_{dipyz\text{-}py}]$

comparing pairs	I		II		III	
formula	$CuCl_2[L^{2py}_{Terpy}]$	$CuCl_2[L^{2py}_{dipyz\text{-}py}]$	$CuCl_2[L^{3py}_{Terpy}]$	$CuCl_2[L^{3py}_{dipyz\text{-}py}]$	$CuCl_2[L^{4py}_{Terpy}]$	$CuCl_2[L^{4py}_{dipyz\text{-}py}]$
α	2.53	14.8	13.03	25.87	38.18	28.02
β	101.91	104.80	107.64	201.35	103.17	105.40
D Cl_{ax}-Hg	2.519	2.464	2.443	2.460	2.579	2.421
D Cl_{eq}-Hg	2.231	2.235	2.218	2.247	2.225	2.225

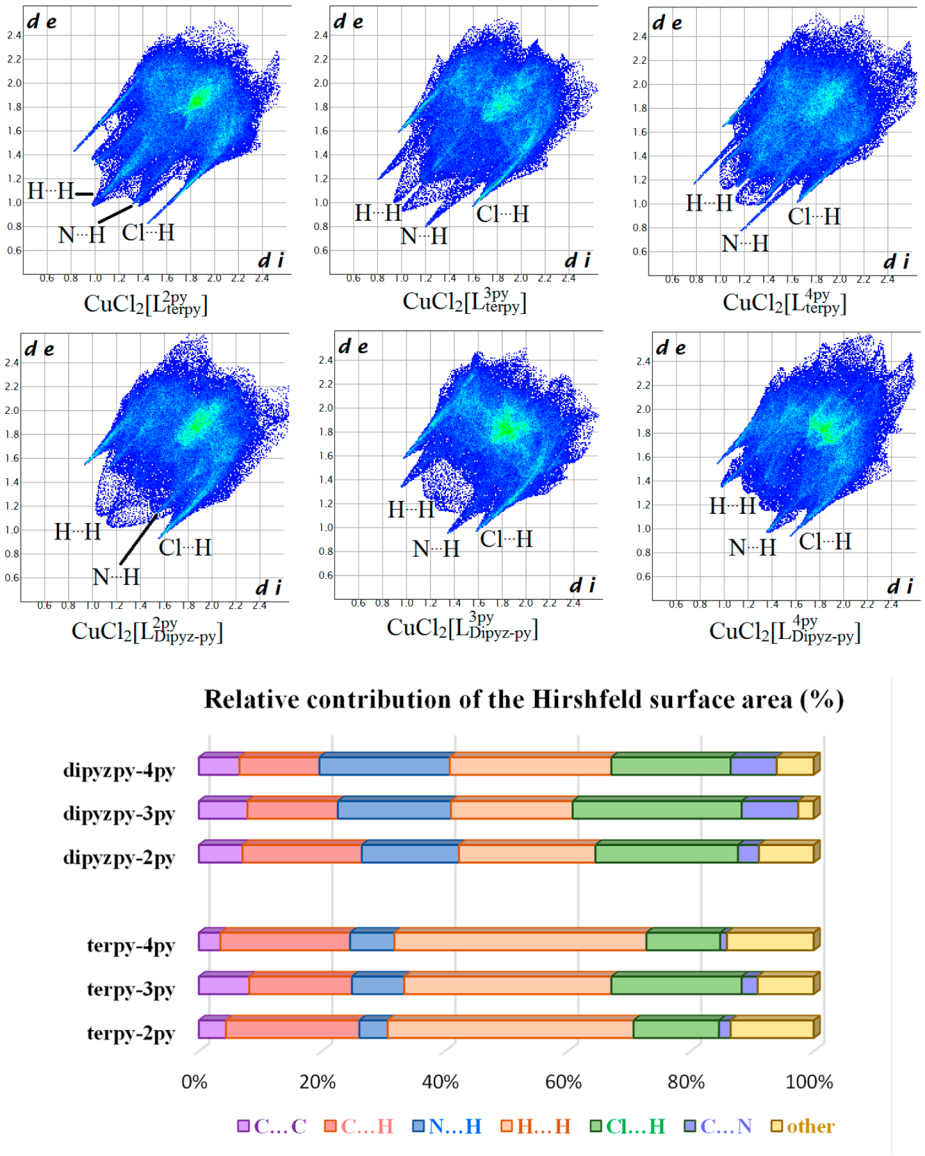

Figure 6. Fingerprint plots (top) and relative contributions of various intermolecular contacts (bottom) relative to the Hirshfeld surface area.

(Refcode: OGOSOT)[33] and **6** (Refcode: EPELIW)[34] were used from the Cambridge Structural Database.[35]

As shown in Figure 1, in all complexes, the coordination geometry around the metal center can be well-defined as slightly distorted square-based pyramide (SBP), with a trigonality index, τ_5,[37] of 0.07, 0.03, 0.15, 0.03, 0.07, and 0.02 for **1**−**6**, respectively. In all structures, the basal plane is occupied by one chloride ion and three nitrogen atoms from the ligand. The apical position is occupied by a chloride ion in normal Cu−Cl distance range of 2.460−2.579 Å.[35] As it is clear from the geometrical parameters around the central metal, Tables S2 and S3, as well as the τ_5 trigonality index values, the Cu(II) ion has a slightly distorted square-based pyramide (SBP) environment in all three complexes.

As it is clear from geometrical parameters, Table S2 and S3, as well as the τ_5 trigonality index values, primary molecular structural studies obtained from single crystals show that the coordination environment around the Cu(II) center in all of the six structures is almost identical. So, different gelation abilities of these compounds cannot be considered as a result of the coordination environment differences, as these differences between gelators and nongelators are slight. On the other hand, different gelation abilities also cannot be related to various geometrical conformations of these complexes as there

DOI: 10.1021/acs.cgd.9b00117
Cryst. Growth Des. XXXX, XXX, XXX−XXX

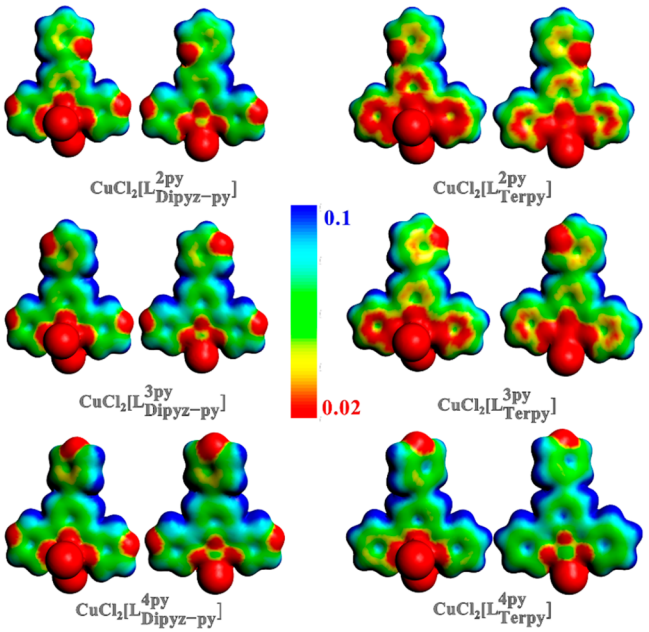

Figure 7. Electrostatic potentials mapped on the electron isodensity surface. The red color shows the most negative potential, while the blue color represents the most positive one.

is no clear trend and regularity between gelation ability and conformation differences. For example, the orientation of the fourth ring in all the structures of this series of components does not have a well-defined routine trend for angles, and we cannot find any correlation with the gelling ability and geometry of molecules. As illustrated in Figure 5, conformational adaptation for the generation of different complexes in this series leads to different angles from 2.53° to 38.18° for two planes of the terpyridine/dipyrazine-pyridine moiety and fourth rings in the crystal arrangement. Pairwise structure comparisons of geometrical parameters of complexes which are listed in Table 1 are in accordance with previous statements. So, molecular structures are similar, but there is little difference between them, and the gelation behavior should be influenced by a factor other than the molecular structure. There are several methods for the comparison of molecular crystal structures. A pairwise Xpac comparison was carried out between the crystal structures of two set complexes. The Xpac dissimilarity index is a quantifiable numeric descriptor for comprising similarities. The smaller the value of *X*, the more equivalent the structure will be. The pairwise comparisons between analogues pair of $CuCl_2[L^{npy}_{Terpy}]$ complexes show that, despite structural differences, there is still a degree of similarity in the structures of these gelators, which can be attributed to the common factor in the formation of the gel of these components. However, this structural similarity between pairs of $CuCl_2[L^{npy}_{Terpy}]$ and $CuCl_2[L^{npy}_{dipyz-py}]$ is not observed. This can then be tracked by the connection between the solid state, and ability to form a gel, which is the next challenging target, is being conducted in our study. Indeed, in order to achieve the design of LMWGs, the crystal engineering approach has confirmed that there is often a correlation between the kind of packing seen in a crystalline state structure of a molecules and their ability to behave as a gelator.[13]

In an attempt to elucidate the origin of these differences, we turned our attention to the molecular arrangement in a single crystal. To visualize and comprehend the intermolecular interactions in the crystalline state, and find logical trends in comparing molecular gelators and nongelators based on solid state interactions, Hirshfeld surface analysis[38] was applied to increase insights into the intermolecular interactions that must play a critical role in the gelation process. For probing the possible role of intermolecular interactions in the gel formation, we discuss the assembly of two closely related analogues of each series and attempt to scrutinize the quality and quantity of interaction by comparing percent relative contribution of the intermolecular interactions in each crystal structure based on Hirshfeld surface analysis and investigate the importance of the presence of this interaction in creating different dimensions in the growth of the 3D network. Fingerprint plots and relative contributions of various intermolecular contacts to the Hirshfeld surface area in related structures are shown in Figure 6. As illustrated in Figure 6, Hirshfeld surface analyses of the pairwise related derivatives of terpyridine and dipyrazine-pyridine analogue structures revealed that there was no regular trend in all of the interactions except the ones that had atoms that are more present in the molecular structure. For example, H···H interaction is more present in the terpyridine analogue because of the existence of more hydrogen atoms in terpyridine analogue than dipyrazine-pyridine counterpart, and it seems quite clear. The only interaction that is outside of this rule is the N···H interaction (the N atom exists more in the dipyrazine-pyridine analogue and the H atom exists more in the terpyridine analogue which balance each other) and Cl···H interaction (shows a reverse trend with existing atoms). The subsequent studies of contribution of interaction showed that the N···H and Cl···H interactions were the important intermolecular interactions affecting organization of the molecules in the solid state.

Although N···H interactions comprise only 4.6% of the Hirshfeld surface in $CuCl_2[L^{2py}_{Terpy}]$, in other cases a considerable contribution of the Hirshfeld surface was accountable for the overall structural property observed in the crystalline state structure. It must be noted that in the $CuCl_2[L^{2py}_{Terpy}]$ (**1**), $CuCl_2[L^{3py}_{Terpy}]$ (**2**), and $CuCl_2[L^{4py}_{Terpy}]$ (**3**), metallogel series, the lower T_{gel} value for **1**, 79 °C, and the higher T_{gel} value for **3**, 83 °C, Figure 2, can be rationally explained based on these N···H, and Cl···H interactions orders.

Furthermore, with less proportion of the surface, N···H hydrogen bonds are somewhat less important than Cl···O for the total stability of the crystal network. We have computed the molecular electrostatic potential (MEP) of compounds **1**−**6** to understand the role of replacing the carbon atom with a nitrogen atom in the terpyridine derivatives (for computational details, see Supporting Information). In the qualitative comparison of the electrostatic potential maps, it is shown that the replacing C−H group with a nitrogen atom exerts variable effects on the negative electrostatic potential of the aromatic ring. From the inspection of the results arises the existence of an electron-withdrawing nitrogen atom leading to dipyzine-pyridine derivatives having substantially lower negative electrostatic potentials on the aromatic rings than the terpyridine counterpart. Thus, we expect more effective hydrogen-bonding interaction with electron-rich terpyridine molecules, Figure 7. Taking into consideration the fact that the terpyridine and dipyrazine-pyridine moieties contain electron-withdrawing atoms that are important in the gelation process, the importance of hydrogen-bonding formation of the overall 3D network is also apparent. Because none of the dipyrazine-

DOI: 10.1021/acs.cgd.9b00117
Cryst. Growth Des. XXXX, XXX, XXX−XXX

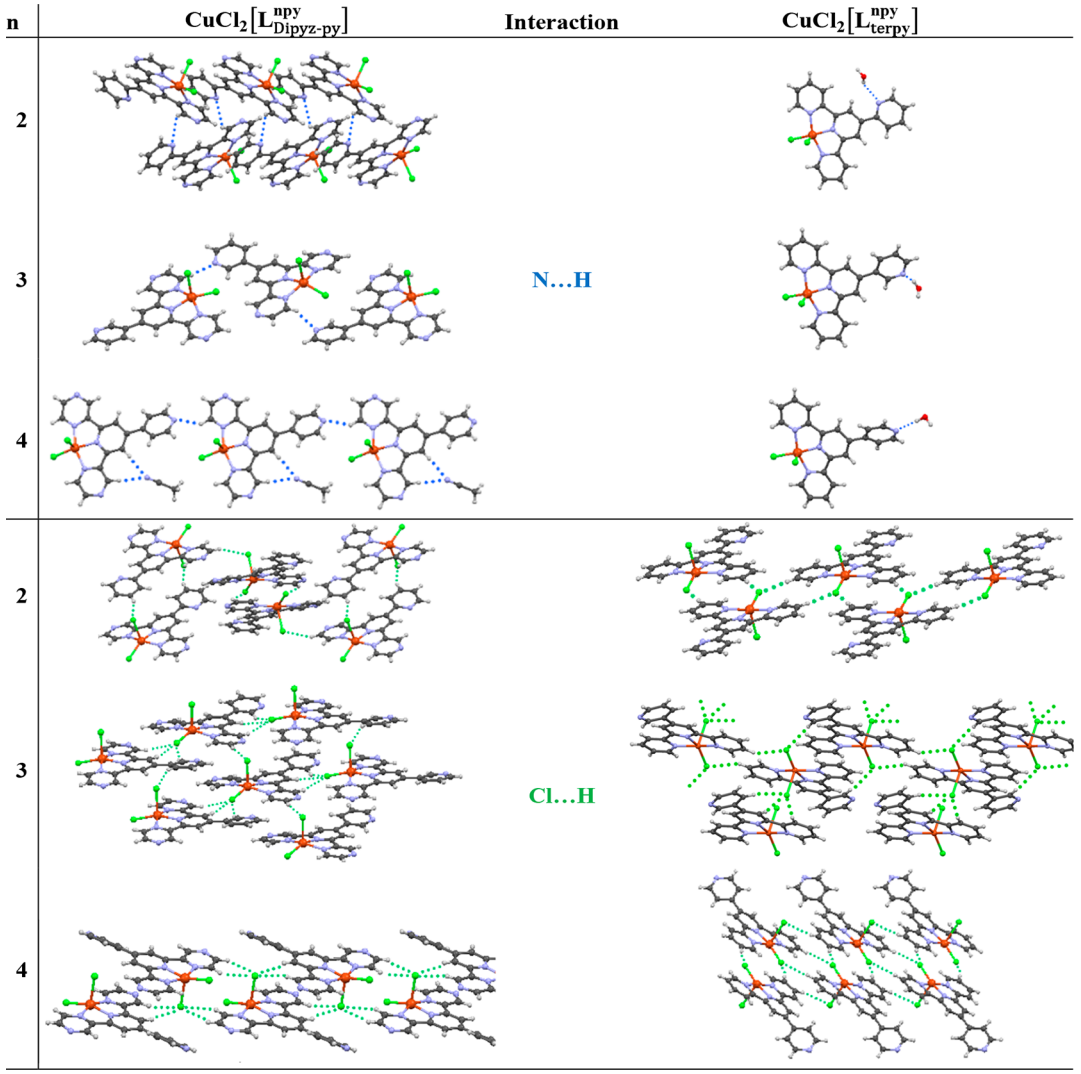

Figure 8. Packing description of N···H and Cl···H interactions in the crystal structure complexes.

pyridine derivatives are devoid of any gelation ability, the origin of being a gelator or not is related to these two interactions. We decided to investigate their role between the terpyridine moieties that might contribute toward gel formation. To obtain insight into the packing mode of the compound, we compared each pair of analogues of two series separately. All of the comparisons reveal that dipyrazine-pyridine analogues have more effective hydrogen-bonding interactions than their terpyridine counterparts (Tables S4 and S5). The highlighting of the aforementioned interaction in the crystal structure of $CuCl_2[L^{npy}_{Terpy}]$ and $CuCl_2[L^{npy}_{dipyz\text{-}py}]$ is shown in Figure 8. In the crystal structure of $CuCl_2[L^{2py}_{Terpy}]$, there is one molecule of complex and two molecules of water in the asymmetric unit. The $CuCl_2[L^{2py}_{Terpy}]$ and water molecules were held together by intermolecular O−H···N and OH···Cl interactions. In comparing in dipyrazine-pyridine counterpart, this interaction is between the nitrogen of the fourth rings and protons of other complexes that aid the formation of an infinite one-dimensional (1D) array of the complex. Similar results were found in the 3py derivate, illustrated in Figure 8. For the dipyrazine-pyridine analogue, the asymmetric unit is formed from the one complex molecule which was stabilized by the hydrogen-bonding intermolecular N···H facilitating the growth of the structure in one direction of the network (Tables S4 and S5). Furthermore, each terpyridine analogue asymmetric unit contains solvent molecules and N. . .H interaction involved trapping solvent in crystal packing. Similarly, these observations were found in the 4py derivative, with this difference that there are two molecules in the asymmetric unit of dipyrazine-pyridine counterpart and one molecule of complex. Each asymmetric unit was involved in two N···H interactions. One of these interactions is between the nitrogen atom of the fourth rings and protons of other complexes, contributing 12.6% of the interactions to the total intermolecular surface close contact interaction, which leads to growth of the crystal structure in one of the directions. The other interaction is between the nitrogen atom of the acetonitrile solvent and the proton of the complex, with 8.5% contribution of the surface being less important. The aforementioned N···H contact is actually part of the 3D formation of the crystal lattice in dipyrazine-pyridine analogues which hampers the production of an appropriate space for the capture of solvent molecules and thus disfavors for the formation of the supramolecular gel. The coordination modes of the Cu atom in terpyridine analogue are similar to those in the dipyrazine-pyridine counterpart. Coordination of three nitrogen atoms two chloride ions results in a distorted square pyramidal Cu(II) metal center. Two coordinated chloride ions in all of the

DOI: 10.1021/acs.cgd.9b00117
Cryst. Growth Des. XXXX, XXX, XXX−XXX

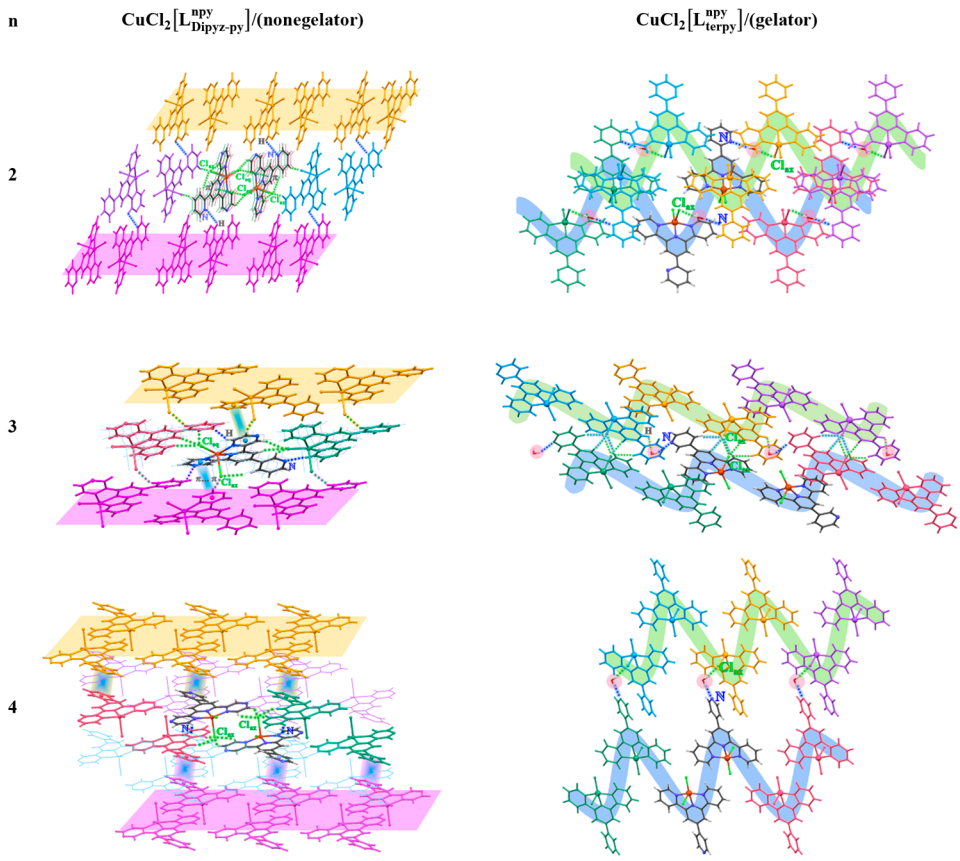

Figure 9. Molecular packing description of gelator and nonegelator in the crystal structure complexes.

dipyrazine-pyridine analogues display hydrogen-bonding interaction. In the case of $CuCl_2[L^{2py}_{dipyz\text{-}py}]$, these hydrogen-bonding interactions result in the formation of a 3D network, Figure 9 and Table S5. In the terpyridine counterpart, coordinated chloride ions are involved in hydrogen bonding that aid in the formation of an infinite one-dimensional array of molecules. The observation of the 3py derivative is very similar to that of 2py derivative except that the Cl···H interaction in terpyridine analogues results in the two-dimensional array of molecules. Different observations were found in the 4py derivative. The Cl···H interaction of two coordinated chlorides in dipyrazine-pyridine analogues led to the formation of a 1D network instead of 3D network and in the terpyridine counterpart. Maybe the origin of this difference is that in spite of our great efforts, we could not obtain a suitable crystal for 4py derivatives from gelling solvents, and crystallographic data have been available and determined from the Cambridge Structural Database.[35] Meanwhile, all the observations reveal that robust intermolecular interactions which contribute to the 3D formation of the network must be one of the key features in this class of compounds to be gelators or nongelators. It is quite interesting to note that in all these structures the N··· H and Cl···H synthon that is observed is more efficient in the dipyrazine-pyridine counterpart as a nongelator compound. The synthon is specified as the structural unit within a supermolecules that can be assembled through known intermolecular interactions. These results are consistent with the idea that nongelators have more effective hydrogen-bonding interactions in the solid state.

Finally, for discerning of molecular packing within gel fibers, the self-assembly properties of each compound were assessed to correlate the gelation ability to the assembly propensity. The self-assembled fibrillar network is made from 1D growth of fibers, so it is logical to believe that anisotropic interactions of the compounds that allow unidirectional growth lead to fibrillar network formation and absence of such interactions in additional two dimensions inhibits the side growth emerging in 1D fibers. From this point of view, it is reasonable to correlate the tendency of the molecules to grow as 1D fibers with supramolecular self-assembly patterns and their gelling or nongelling behavior. The presence of such chains, rather than layers, seems to be very important in gel formation. It is essential to recognize supramolecular synthons that are so sturdy to guarantee their their repetitivity and generality in the resulting gel network formation. The concept of robustness of the supramolecular synthon is represented with the packing description of these related compounds in Figure 9. As illustrated in this diagram, the frequently occurring 1D chain formation by Cl···H hydrogen bonding in the gelator molecule shows that the hydrogen-bonded network of equatorial chloride was found to be the key interaction in the 1D growth of the fiber. All crystal structures presented 1D hydrogen-bonded networks in both gelator and nongelator components, while a 1D chain in the nongelator is carried out by other robust supramolecular synthons requiring two additional dimensions which are responsible for the 3D network formation thereby being unable to create 1D fibers, so resulting in nongelators. Lack of such robust intermolecular interactions contributes to the stability of the 1D network in gelators compared to that in nongelators following the formation of the gel. In the gel phase, the solvation must compete with the intermolecular interaction, and the fibrous

DOI: 10.1021/acs.cgd.9b00117
Cryst. Growth Des. XXXX, XXX, XXX−XXX

structure must be so secure as it ultimately prevents the 3D insoluble aggregates. In the crystal structure of gelators, the 1D chain is joined by mediation of solvent molecules into 2D layers. As a result, solvent molecules are trapped in the cross-linked network of the fibers, and the 3D hydrogen-bonding network in the nongelators leads them to not act as a gelator and shows lower solubility than the gelators which constructs the 1D hydrogen-bonding array.

The aforementioned results clearly demonstrate that both strategies to approach the gelation phenomenon from a microscopic and macroscopic viewpoint contribute to a better comprehension of the process of how small molecules gelate solvents. On the basis of these results, the possible mechanism for inhibiting the formation of hydrogels can be proposed, as a robust supramolecular synthon prevents the one-dimensional alignment of molecules. These considerations are accordance with the contrast in the formation of crystals versus formation of a fiber, whereby the intermolecular interactions within a fiber are identified to be aligned, thus promoting 1D growth, whereas in the crystal structure they are aligned to multiple axes providing 3D growth.

CONCLUSION

Current investigations are ongoing to correlate the molecular structure to the gelation ability by analysis of the molecular arrangement in the single crystal. We have reported that closely related molecules bear very different abilities to form gels;[39−43] indeed, an uncomplicated variation in the structure of the molecule can induce extreme variations in the gelation ability. This is highlighted again by the results presented here. We have shown that two sets of structurally similar molecules, one of which is unable to form a gel and the other set can form a metastable gel. To investigate the basis for these variations, we have used Hirshfeld surface analysis and examined differences in their packing arrangements, which suggests that hydrogen bonding arranged into the 3D network is a preferred mode of packing for the crystalline solid but is unfavorable for gel formation. Of course, we completely realize that there are some exceptions to this methodology, but this is very beneficial to efficiently predict gelation ability and skillfully design good gelators.

ASSOCIATED CONTENT

Supporting Information

This material is free of charge via Internet at The Supporting Information is available free of charge on the ACS Publications website at DOI: 10.1021/acs.cgd.9b00117.

Synthetic procedures, crystallographic data, selected bond distance and angles, hydrogen-bonding interaction data (PDF)

Accession Codes

CCDC 1883949−1883952 (**1**, **2**, **4**, and **5**) contain the supplementary crystallographic data for this paper. These data can be obtained free of charge via www.ccdc.cam.ac.uk/data_request/cif, or by emailing data_request@ccdc.cam.ac.uk, or by contacting The Cambridge Crystallographic Data Centre, 12 Union Road, Cambridge CB2 1EZ, UK; fax: +44 1223 336033.

AUTHOR INFORMATION

Corresponding Author

*Tel. No: +98 21 29903105. Fax No.: +98 21 22431661. E-mail: khavasihr@gmail.com.

ORCID

Hamid Reza Khavasi: 0000-0003-2303-3668

Notes

The authors declare no competing financial interest.

ACKNOWLEDGMENTS

We would like to thank the Graduate Study Councils of Shahid Beheshti University, General Campus, and the Iran National Science Foundation (Grant No. 940090) for financial support.

REFERENCES

(1) Hirst, A. R.; Escuder, B.; Miravet, J. F.; Smith, D. K. High-Tech Applications of Self-Assembling Supramolecular Nanostructured Gel-Phase Materials: From Regenerative Medicine to Electronic Devices. *Angew. Chem., Int. Ed.* **2008**, *47*, 8002−8018.

(2) Banerjee, S.; Das, R. K.; Maitra, U. Supramolecular Gels 'in Action.'. *J. Mater. Chem.* **2009**, *19*, 6649−6687.

(3) Piepenbrock, M.-O. M.; Lloyd, G. O.; Clarke, N.; Steed, J. W. Metal- and Anion-Binding Supramolecular Gels. *Chem. Rev.* **2010**, *110*, 1960−2004.

(4) Dawn, A.; Shiraki, T.; Haraguchi, S.; Tamaru, S.; Shinkai, S. What Kind of "Soft Materials" Can We Design from Molecular Gels? *Chem. - Asian J.* **2011**, *6*, 266−282.

(5) Raeburn, J.; Zamith Cardoso, A.; Adams, D. J. The Importance of the Self-Assembly Process to Control Mechanical Properties of Low Molecular Weight Hydrogels. *Chem. Soc. Rev.* **2013**, *42*, 5143−5156.

(6) Segarra-Maset, M. D.; Nebot, V. J.; Miravet, J. F.; Escuder, B. Control of Molecular Gelation by Chemical Stimuli. *Chem. Soc. Rev.* **2013**, *42*, 7086−7098.

(7) Adarsh, N. N.; Kumar, D. K.; Dastidar, P. Composites of N,N'-Bis-(Pyridyl) Urea-Dicarboxylic Acid as New Hydrogelators-a Crystal Engineering Approach. *Tetrahedron* **2007**, *63*, 7386−7396.

(8) Wang, H.; Shi, Y.; Wang, L.; Yang, Z. Recombinant Proteins as Cross-Linkers for Hydrogelations. *Chem. Soc. Rev.* **2013**, *42*, 891−901.

(9) Yu, G.; Yan, X.; Han, C.; Huang, F. Characterization of Supramolecular Gels. *Chem. Soc. Rev.* **2013**, *42*, 6697−6722.

(10) Babu, S. S.; Praveen, V. K.; Ajayaghosh, A. Functional π-Gelators and Their Applications. *Chem. Rev.* **2014**, *114*, 1973−2129.

(11) Dastidar, P.; Ganguly, S.; Sarkar, K. Metallogels from Coordination Complexes, Organometallic, and Coordination Polymers. *Chem. - Asian J.* **2016**, *11*, 2484−2498.

(12) Samai, S.; Biradha, K. Chemical and Mechano Responsive Metal−Organic Gels of Bis(benzimidazole)-Based Ligands with Cd(II) and Cu(II) Halide Salts: Self Sustainability and Gas and Dye Sorptions. *Chem. Mater.* **2012**, *24*, 1165−1173.

(13) Dastidar, P. Supramolecular Gelling Agents: Can They Be Designed? *Chem. Soc. Rev.* **2008**, *37*, 2699−2715.

(14) Chen, J.; Kampf, J. W.; McNeil, A. J. Comparing Molecular Gelators and Nongelators Based on Solubilities and Solid-State Interactions. *Langmuir* **2010**, *26*, 13076−13080.

(15) Adarsh, N. N.; Sahoo, P.; Dastidar, P. Is a Crystal Engineering Approach Useful in Designing Metallogels? A Case Study. *Cryst. Growth Des.* **2010**, *10*, 4976−4986.

(16) Wang, J.; Liu, K.; Xing, R.; Yan, X. Peptide Self-Assembly: Thermodynamics and Kinetics. *Chem. Soc. Rev.* **2016**, *45*, 5589−5604.

(17) Tomasini, C.; Castellucci, N. Peptides and Peptidomimetics That Behave as Low Molecular Weight Gelators. *Chem. Soc. Rev.* **2013**, *42*, 156−172.

(18) Ramos Sasselli, I.; Halling, P. J.; Ulijn, R. V.; Tuttle, T. Supramolecular Fibers in Gels Can Be at Thermodynamic

DOI: 10.1021/acs.cgd.9b00117
Cryst. Growth Des. XXXX, XXX, XXX−XXX

Equilibrium: A Simple Packing Model Reveals Preferential Fibril Formation *versus* Crystallization. *ACS Nano* **2016**, *10*, 2661−2668.
(19) Sambri, L.; Cucinotta, F.; Paoli, G.; Stagni, S.; De Cola, L. Ultrasound-Promoted Hydrogelation of Terpyridine Derivatives. *New J. Chem.* **2010**, *34*, 2093−2096.
(20) Tam, A. Y.-Y.; Wong, K. M.-C.; Yam, V. W.-W. Influence of Counteranion on the Chiral Supramolecular Assembly of Alkynylplatinum(II) Terpyridyl Metallogels That Are Stabilised by Pt···Pt and π-π Interactions. *Chem. - Eur. J.* **2009**, *15*, 4775−4778.
(21) Gasnier, A.; Royal, G.; Terech, P. Metallo-Supramolecular Gels Based on a Multitopic Cyclam Bis-Terpyridine Platform †. *Langmuir* **2009**, *25*, 8751−8762.
(22) Tatikonda, R.; Bhowmik, S.; Rissanen, K.; Haukka, M.; Cametti, M. Metallogel Formation in Aqueous DMSO by Perfluoroalkyl Decorated Terpyridine Ligands. *Dalt. Trans.* **2016**, *45*, 12756−12762.
(23) Tam, A. Y.-Y.; Wong, K. M.-C.; Wang, G.; Yam, V. W.-W. Luminescent Metallogels of Platinum(II) Terpyridyl Complexes: Interplay of Metal···metal, $\pi - \pi$ and Hydrophobic−hydrophobic Interactions on Gel Formation. *Chem. Commun.* **2007**, 2028−2030.
(24) Hanabusa, K.; Hirata, T.; Inoue, D.; Kimura, M.; Shirai, H. Formation of Physical Hydrogels with Terpyridine-Containing Carboxylic Acids. *Colloids Surf., A* **2000**, *169*, 307−316.
(25) Bhowmik, S.; Ghosh, B. N.; Rissanen, K. Transition Metal Ion Induced Hydrogelation by Amino-Terpyridine Ligands. *Org. Biomol. Chem.* **2014**, *12*, 8836−8839.
(26) Camerel, F.; Ziessel, R.; Donnio, B.; Guillon, D. Engineering of an Iron−terpyridine Complex with Supramolecular Gels and Mesomorphic Properties. *New J. Chem.* **2006**, *30*, 135−139.
(27) Bhowmik, S.; Ghosh, B. N.; Marjomäki, V.; Rissanen, K. Nanomolar Pyrophosphate Detection in Water and in a Self-Assembled Hydrogel of a Simple Terpyridine-Zn^{2+}Complex: A Case Study. *J. Am. Chem. Soc.* **2014**, *136*, 5543−5546.
(28) Laxmi Madhavi, N. N.; Bilton, C.; Howard, J. A. K.; Allen, F. H.; Nangia, A.; Desiraju, G. R. Seeking Structural Repetitivity in Systems with Interaction Interference: Crystal Engineering in the Gem-Alkynol Family. *New J. Chem.* **2000**, *24*, 1−4.
(29) Desiraju, G. R. Crystal Engineering: A Holistic View. *Angew. Chem., Int. Ed.* **2007**, *46*, 8342−8356.
(30) van Bommel, K. J. C.; van der Pol, C.; Muizebelt, I.; Friggeri, A.; Heeres, A.; Meetsma, A.; Feringa, B. L.; van Esch, J. Responsive Cyclohexane-Based Low-Molecular-Weight Hydrogelators with Modular Architecture. *Angew. Chem.* **2004**, *116*, 1695−1699.
(31) Estroff, L. A.; Hamilton, A. D. Water gelation by small organic molecules. *Chem. Rev.* **2004**, *104*, 1201−1218.
(32) Terech, P.; Weiss, R. G. Low molecular mass gelators of organic liquids and the properties of their gels. *Chem. Rev.* **1997**, *97*, 3133−3160.
(33) Beves, J. E.; Constable, E. C.; Decurtins, S.; Dunphy, E. L.; Housecroft, C. E.; Keene, T. D.; Neuburger, M.; Schaffner; Zampese, J. A. Structural diversity in the reactions of 4'-(pyridyl)-2, 2': 6', 2 ″-terpyridine ligands and bis {4'-(4-pyridyl)-2, 2': 6', 2 ″-terpyridine} iron (II) with copper (II) salts. *CrystEngComm* **2009**, *11*, 2406−2416.
(34) Miller, R. G.; Brooker, S. Spin crossover, reversible redox, and supramolecular interactions in 3d complexes of 4-(4-pyridyl)-2, 5-dipyrazyl-pyridine. *Inorg. Chem.* **2015**, *54*, 5398−5409.
(35) *Cambridge Structural Database*, version 5.39; CCDC: Cambridge, U.K., 2018.
(36) Wang, J.; Hanan, G. A Facile Route to Sterically Hindered and Non-Hindered 4'-Aryl-2,2':6',2''-Terpyridines. *Synlett* **2005**, *2005*, 1251−1254.
(37) Addison, A. W.; Rao, T. N.; Reedijk, J.; Van Rijn, J.; Verschoor, G. C. Synthesis, structure, and spectroscopic properties of copper(II) compounds containing nitrogen−sulphur donor ligands; the crystal and molecular structure of aqua [1,7-bis(N-methylbenzimidazol-2'-yl)-2,6-dithiaheptane]copper(II) perchlorate. *J. Chem. Soc., Dalton Trans.* **1984**, 1349−1356.
(38) Spackman, M. A.; Jayatilaka, D. Hirshfeld surface analysis. *CrystEngComm* **2009**, *11*, 19−32.
(39) Adams, D. J.; Morris, K.; Chen, L.; Serpell, L. C.; Bacsa, J.; Day, G. M. The Delicate Balance between Gelation and Crystallisation: Structural and Computational Investigations. *Soft Matter* **2010**, *6*, 4144−4156.
(40) de Loos, M.; van Esch, J. H.; Kellogg, R. M.; Feringa, B. L. C3-Symmetric, Amino Acid Based Organogelators and Thickeners: A Systematic Study of Structure−property Relations. *Tetrahedron* **2007**, *63*, 7285−7301.
(41) Yang, Z.; Liang, G.; Ma, M.; Gao, Y.; Xu, B. Conjugates of Naphthalene and Dipeptides Produce Molecular Hydrogelators with High Efficiency of Hydrogelation and Superhelical Nanofibers. *J. Mater. Chem.* **2007**, *17*, 850−854.
(42) Ma, M.; Kuang, Y.; Gao, Y.; Zhang, Y.; Gao, P.; Xu, B. Aromatic-Aromatic Interactions Induce the Self-Assembly of Pentapeptidic Derivatives in Water To Form Nanofibers and Supramolecular Hydrogels. *J. Am. Chem. Soc.* **2010**, *132*, 2719−2728.
(43) Kumar, K. K.; Elango, M.; Subramanian, V.; Das, T. M. Novel Saccharide−pyridine Based Gelators: Selective Gelation and Diversity in Superstructures. *New J. Chem.* **2009**, *33*, 1570−1577.

DOI: 10.1021/acs.cgd.9b00117
Cryst. Growth Des. XXXX, XXX, XXX−XXX